© 2013. Published by The Company of Biologists Ltd | Development (2013) 140, 4797-4806 doi:10.1242/dev.094979

RESEARCH ARTICLE

Guidance receptor promotes the asymmetric distribution of exocyst and recycling endosome during collective cell migration

Ping Wan[1], Dou Wang[1], Jun Luo[1], Dandan Chu[1,2], Heng Wang[1], Lijun Zhang[1] and Jiong Chen[1,3,*]

ABSTRACT

During collective migration, guidance receptors signal downstream to result in a polarized distribution of molecules, including cytoskeletal regulators and guidance receptors themselves, in response to an extracellular gradient of chemotactic factors. However, the underlying mechanism of asymmetry generation in the context of the migration of a group of cells is not well understood. Using border cells in the *Drosophila* ovary as a model system for collective migration, we found that the receptor tyrosine kinase (RTK) PDGF/VEGF receptor (PVR) is required for a polarized distribution of recycling endosome and exocyst in the leading cells of the border cell cluster. Interestingly, PVR signaled through the small GTPase Rac to positively affect the levels of Rab11-labeled recycling endosomes, probably in an F-actin-dependent manner. Conversely, the exocyst complex component Sec3 was required for the asymmetric localization of RTK activity and F-actin, similar to that previously reported for the function of Rab11. Together, these results suggested a positive-feedback loop in border cells, in which RTKs such as PVR act to induce a higher level of vesicle recycling and tethering activity in the leading cells, which in turn enables RTK activity to be distributed in a more polarized fashion at the front. We also provided evidence that E-cadherin, the major adhesion molecule for border cell migration, is a specific cargo in the Rab11-labeled recycling endosomes and that Sec3 is required for the delivery of the E-cadherin-containing vesicles to the membrane.

KEY WORDS: Collective cell migration, Exocyst, Guidance receptor, Rab11, Recycling endosome, Sec3, *Drosophila*

INTRODUCTION

During chemotaxis, migrating cells are often guided by external guidance cues, which are probably distributed in a graded fashion along the migratory route. Upon sensing such an extracellular gradient, the guidance receptors of migratory cells signal intracellularly to convert a usually shallow external gradient of guidance cues into a robust intracellular front-back polarity, which is essential for chemotactic migration of individual cells (Devreotes and Janetopoulos, 2003). However, cells do not always migrate individually; they often migrate collectively as a cluster, a sheet or a strand of cells in physiological, developmental and cancer metastatic conditions (Friedl and Gilmour, 2009; Rørth, 2011). During collective cell migration, each group of either tightly connected or loosely associated cells also needs to interpret an external gradient of chemotactic factors and convert it into a strong front-back asymmetry across a collective group rather than an individual cell, which is often manifested as one cell in the leading edge extending a protrusion and leading the rest of group forward (Friedl and Gilmour, 2009; Rørth, 2011). Both single cell migration and collective migration require a strong amplification process that results in an asymmetric distribution of cytoskeletal and adhesive molecules within an individual cell or within a group of cells, but the underlying mechanism is not clearly understood. Recently, evidence began to emerge pointing to intracellular trafficking as a probable mechanism for such amplification.

Endocytosis is a common mechanism employed by eukaryotic cells to internalize extracellular materials, receptors and other proteins and lipids in the plasma membrane (Grant and Donaldson, 2009; Maxfield and McGraw, 2004). The endocytic vesicles containing these cargoes first fuse with the early endosome or sorting endosome, where the proteins and lipids are then sorted for transport via different routes. They are either transported to the late endosome and then lysosome for degradation or recycled back to the plasma membrane via the recycling endosome. Previous studies have shown that the endocytic pathway is crucial for both individual and collective cell migration. For example, tissue cell culture experiments demonstrated that during single cell migration, internalization and recycling of integrin not only promotes the dynamic disassembly and assembly of adhesive contacts, but also restricts the localization of integrin to the front of the cell (Caswell and Norman, 2008; Caswell et al., 2007; Ulrich and Heisenberg, 2009). This is probably achieved when localized endocytic recycling of integrin at the leading edge outcompete the slow lateral diffusion of integrin toward the cell body.

Similarly, during collective migration of *Drosophila* border cells, endocytic recycling was shown by several studies to be required for restricting phosphotyrosine [pTyr, a measurement of receptor tyrosine kinase (RTK) activity] to the leading edge of each migrating cell cluster (Assaker et al., 2010; Janssens et al., 2010). During *Drosophila* oogenesis, a coherent cluster of about eight border cells delaminate from the anterior follicle epithelium and migrate collectively through the germline-derived nurse cells of a stage-9 egg chamber (Fig. 1A). The stereotypic and directed migration of border cells are guided by several external guidance cues secreted from the posteriorly located oocyte, acting on two RTKs, PDGF/VEGF receptor (PVR) and Epidermal growth factor receptor (EGFR), to transduce guidance signaling. It has been shown that dynamin and other regulators of the early steps of endocytosis, including a guanine exchange factor for Rab5 (promoting cargo entry into early endosome), were involved in localizing pTyr to the front of border cell clusters (Jékely et al., 2005). In addition, Rab11 (a positive regulator of recycling endosome) and its effector, the exocyst component Sec15, were also shown to be required for the asymmetric localization of pTyr (Assaker et al., 2010; Janssens et al., 2010).

[1]Model Animal Research Center, and MOE Key Laboratory of Model Animals for Disease Study, Nanjing University, Nanjing, China 210061. [2]Jiangsu Key Laboratory of Neuroregeneration, Nantong University, Nantong, China 226001. [3]Zhejiang Key Laboratory for Technology and Application of Model Organisms, School of Life Sciences, Wenzhou Medical College, Wenzhou, China 325035.

*Author for correspondence (chenjiong@nju.edu.cn)

Received 8 February 2013; Accepted 13 September 2013

Development (2013) doi:10.1242/dev.094979

Based on these studies, it had been suggested that there might be a directional recycling of active RTKs to the leading edge of border cells, amplifying the initial small difference between RTK signaling levels at the front and those at the back (Janssens et al., 2010; Jékely et al., 2005; Montell et al., 2012). Recently, it was shown that the active (tyrosine phosphorylated) form of PVR was enriched at the front of cluster when PVR is overexpressed, but the front-back asymmetry of active PVR is significantly less than that of pTyr. This discrepancy raises the question of whether kinases and phosphorylated proteins other than active PVR are directionally recycled to the front. Moreover, how this recycling process is regulated is unclear. In this study, we showed that there was a polarized distribution of Rab11-labeled recycling endosome and Sec5-labeled exocyst near the leading edge of migrating border cells, which is mediated by the guidance receptor PVR. Interestingly, we found PVR signaled through the small GTPase Rac to locally increase recycling endosome levels. Elevated recycling endosome levels were proximal to strong F-actin stainings, which normally occurred at the leading edge of the migrating cluster, suggesting that directional recycling could be mediated by the asymmetrically localized F-actin. Conversely, the exocyst component Sec3 was also required for asymmetric localization of RTK activity and F-actin. These results suggested the presence of a positive feedback loop in border cells, where RTKs such as PVR acted to induce a higher level of vesicle recycling and tethering activity in the leading cells, enabling active RTKs or other phosphorylated proteins to be concentrated in a more polarized fashion at the front. Lastly, we also provided evidence that Sec3 promoted recycling and tethering of vesicles containing E-cadherin (Shotgun – FlyBase) in border cells and follicle cells.

RESULTS

Sec 3 is required for border cell migration

In a search for genes essential for border cell migration, we screened a collection of flippase (Flp) recognition target (FRT)-P-element lethal mutations described previously (Chen et al., 2005). Using genetic mosaic methods (Flp-*FRT*), we identified a P-element line, 10199, that displayed border cell migration defects. Detailed genetic analyses including P-element excision, deficiency mapping and DNA sequencing, had uncovered that the defects were not caused by the P-element insertion but by a point mutation in the CG3885 locus, which encodes the *Drosophila* homolog of Sec3, an exocyst component that had not been genetically characterized in *Drosophila* (Boyd et al., 2004; Finger et al., 1998; He and Guo, 2009). The exocyst is a complex composed of eight subunits, which were shown to mediate the tethering of secretory or recycling vesicles to the plasma membrane before the step of exocytic fusion during various polarized cellular processes in yeast, *Drosophila* and mammals (Finger et al., 1998; He and Guo, 2009; Langevin et al., 2005). The isolated allele was named $sec3^{GT}$ because of the G to T mutation that disrupts the stop codon (supplementary material Fig. S1A), and it failed to complement a lethal PiggyBac insertional allele of *sec3* ($sec3^{PBac}$). Both alleles were shown to be loss-of-function alleles, as the homozygous mutants died at third instar larval stage and displayed strong reduction of sec3 RNA levels compared with the wild type (supplementary material Fig. S1). A *sec3* cDNA construct expressed by *UAS/Gal4* system was able to rescue the larval lethality for both alleles, indicating they were bona fide *sec3* mutations (supplementary material Table S1). Lastly, expressing *sec3* RNAi in the border cell clusters by *c306-Gal4* produced similar migration defects (Fig. 1D,F).

Detailed phenotypic analyses showed that mosaic border cell clusters containing clones mutant for either $sec3^{GT}$ or sec^{PBac} displayed significant migration delay. In wild-type stage-10 egg chambers, almost all (97%) of the border cell clusters reached the oocyte border, whereas 35% ($sec3^{GT}$) or 43% (sec^{PBac}) of the mutant mosaic border cell clusters failed to reach the border by stage 10 (Fig. 1B,C,F). A significant percentage of these delayed border cell clusters stopped at the starting point of the migration route (Fig. 1F). Furthermore, we found that within the mosaic border cell clusters *sec3* mutant cells tended to stay at the lagging end, whereas the heterozygous border cells tended to stay at the leading edge (Fig. 1E,E′,G). By contrast, increasing *sec3* expression in a single border cell enabled it to become much more likely to be a leading cell within a cluster (supplementary material Fig. S2). Together, these data indicate that Sec3 promotes both the collective migration of border cell clusters and the leading ability of individual border cells.

Sec 3 is required for pTyr and F-actin asymmetry

A prominent feature of guided migration of a border cell cluster is the presence of a polarized lamellipodial protrusion that is rich in F-actin and is extended by one or two border cells at the leading edge. Such a polarization of F-actin within the border cell clusters was lost in *sec3* mutant or RNAi knockdown clusters, and large lamellipodial protrusions were rarely observed at the leading edge (Fig. 2A-C). This result suggests that the overall front-back polarity of border cell clusters was affected. Indeed, *sec3* mutant or RNAi border cell clusters displayed an absence of front-back asymmetry of pTyr staining, which has been validated as a reliable local readout of endogenous RTK activity levels within border cell clusters (Assaker et al., 2010; Jékely et al., 2005). In these clusters, pTyr staining was somewhat uniform, whereas it was strongly enriched at the front of the wild-type border cell cluster (Fig. 2A,B,D). Consistently, recent work had shown that front-back polarity of pTyr staining was similarly disrupted in *sec15* RNAi border cells, and RNAi knockdown of *sec15* and three other genes encoding some of the subunits (*sec5*, *sec6*, *sec8*) of exocyst complex also displayed migration defects (Assaker et al., 2010). It should be noted that front-back asymmetry of F-actin and pTyr is most prominent during early phase of border cell migration, during later phase this asymmetry is moderate but still significant (supplementary material Fig. S3A′ and Fig. S4B,D), hence the above data have all been collected on clusters initiating migration. Together, these data indicate that Sec3 or the exocyst complex as a whole is required for front-back polarity of RTK signaling and F-actin in border cell clusters.

Guidance receptors are required for asymmetric distribution of Sec5 and Rab 11

Previous works had suggested that endocytic recycling was involved in enriching pTyr in the leading edge of border cell clusters (Assaker et al., 2010; Janssens et al., 2010). As components of exocyst have been shown to interact with Rab11 (Beronja et al., 2005; Langevin et al., 2005; Wu et al., 2005; Zhang et al., 2004), a major marker of recycling endosomes, we decided to determine the distribution patterns of exocyst and Rab11 within the border cell clusters. A Rab11-GFP transgene (expressed by *slbo-Gal4*) has been previously reported to display no obvious front bias in border cells (Assaker et al., 2010). However, we found that a specific antibody against Rab11 (shown to be specific for endogenous Rab11 in supplementary material Fig. S3A-D′) revealed a clear front-back asymmetry of endogenous Rab11 within border cell clusters (Fig. 3A,A′); the front-back ratio was measured to be 1.80±0.12 (n=16)

Development (2013) doi:10.1242/dev.094979

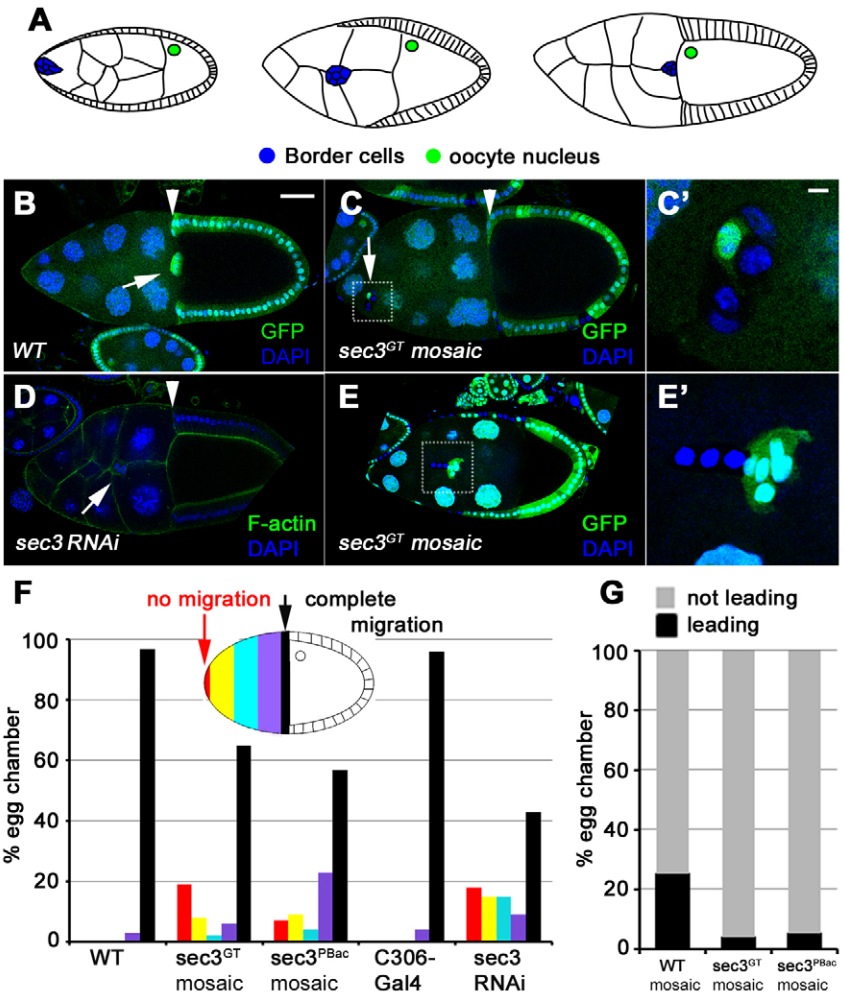

Fig. 1. Sec3 is required for border cell migration. (A) A diagram of border cell migration. (B) A wild-type border cell cluster reaches the oocyte in a stage-10 egg chamber. The arrow points to the border cell cluster, reaching the border between nurse cells and oocyte, as indicated by the arrowhead. (C,C′) A *sec3*^{GT} mosaic border cell cluster fails to migrate to the border at stage 10. (C′) A magnified view of the mosaic cluster, as outlined in the white box in C. A clone of mutant cells is marked by the absence of green fluorescent protein (GFP); a heterozygous cell is marked by GFP. (D) Expression of *UAS-sec3* RNAi driven by *c306-GAL4* delayed border cell migration. (E) An example of *sec3*^{GT} mosaic clusters with mutant cells lagging behind, with an enlarged view of the cluster in E′. Migration direction is to the right in this and all subsequent figures. (F) Quantification of border cell migration in wild-type, *sec3* mosaic, *UAS-sec3* RNAi expressing (driven by *c306*-GAL4) stage-10 egg chambers ($40<n<60$ for each genotype). The extent of migration for all stage-10 egg chambers examined is measured as 0-5% (red, no migration), 6-25% (yellow), 26-50% (blue), 51-75% (purple), 76-100% (black, complete migration). For example, in 97% of wild-type egg chambers, border cells have reached the border (at 76-100% migration distance). (G) Wild-type clones within mosaic clusters are more likely (25% of the time) to occupy the leading position in the cluster than *sec3* mutant clones (4% for *sec*^{GT}, 5% for *sec*^{PBac}) ($47<n<60$). Scale bars: 50 μm in B-E; 5 μm in C′,E′. WT, wild type.

by fluorescence quantification (Fig. 3I). In addition, a different Rab11-GFP transgene (different from the above one and obtained from the Bloomington Stock Center, stock# 8506) expressed in border cells by *slbo-Gal4* gave a similar asymmetric staining pattern as the Rab11 antibody (supplementary material Fig. S4), confirming the antibody staining result. Note that all front-back ratios described here were measured for clusters undergoing the first phase of migration (0-50% position); a lower but significant asymmetry for Rab11 and Rab11-GFP was also detected for clusters during the second half of migration (50-100%; supplementary material Fig. S4). Interestingly, immunostaining using a well-documented Sec5 (an exocyst subunit) (Beronja et al., 2005; Langevin et al., 2005; Murthy et al., 2003; Murthy et al., 2010) antibody, also uncovered a similar front-back ratio of 1.80±0.15 (n=16) in its distribution pattern (Fig. 3E,E′,J). Both Rab11 and Sec5 were shown to be enriched near the leading edge (Fig. 3A′,E′).

We next tested the possibility that the asymmetry of Rab11 and Sec5 was regulated by the guidance signaling. Remarkably, front-back ratios of both Rab11 and Sec5 were reduced to 1.13±0.03 (n=16) and 1.0±0.03 (n=15), respectively, in border cells expressing the dominant-negative forms of both PVR and EGFR (DN-PVR + DN-EGFR, Fig. 3B′,F′,I,J) by *slbo-Gal4*, which effectively removed directional guidance in border cells (Duchek et al., 2001; Prasad and Montell, 2007). Furthermore, expressing DN-PVR alone resulted in a strong reduction of front-back ratios for both Rab11 (1.25±0.04, n=13) and Sec5 (1.17±0.09, n=13), whereas DN-EGFR expression resulted in no significant reduction (Fig. 3C′,G′,I,J), suggesting that PVR is the major RTK that mediated their polarization. Interestingly, expressing a constitutive active form of PVR (λ-PVR) (Duchek et al., 2001) in all outer border cells also caused a remarkable reduction of front-back ratios for Rab11 and Sec5 (Fig. 3D′,H′-J), accompanied by a complete block of migration (data not shown) (Duchek et al., 2001; Zhang et al., 2011); however, the overall levels of Rab11 (but not Sec5) were significantly elevated (Fig. 3D′,H′; Fig. 4K; quantification data not shown for Sec5). By contrast, λ-EGFR (Queenan et al., 1997) expression resulted in no effects on the front-back ratio or the overall levels of Rab11 (Fig. 3I,J; Fig. 4K). Lastly, to show that this loss of asymmetry is specific for disruption of guidance and not merely a consequence of just any migration delay, we demonstrated that deficiency in either Rho1 (the RhoGTPase) or Par-1 (epithelial polarity regulator) resulted in no reduction of Rab11 asymmetry but significant migration delay (Fig. 4J,M; supplementary material Fig. S5). Taken together, these results suggested that the guidance signaling in response to graded chemotactic factors caused a polarized vesicle recycling and tethering activity.

PVR acts through Rac to affect recycling endosome level and organization

The above data on λ-PVR suggest that PVR signals increase recycling endosome levels. To further test this hypothesis, we overexpressed PVR or λ-PVR in follicle cells by *slbo-Gal4*, which

Development (2013) doi:10.1242/dev.094979

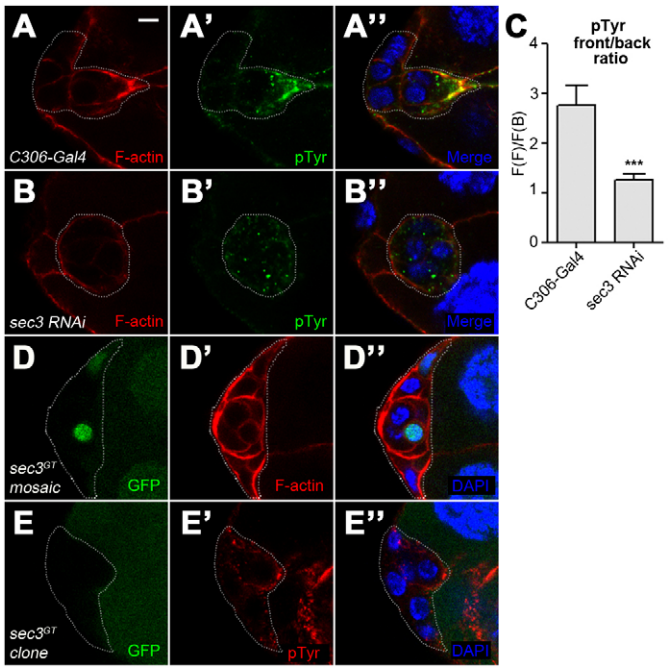

Fig. 2. Sec 3 is required for p-Tyr and F-actin asymmetry. (A-A″) A wild-type border cell cluster shows polarized F-actin and pTyr stainings at the front. (B-B″) A *sec3*-RNAi-expressing (by *c306-Gal4*) border cell cluster does not have polarized F-actin and pTyr stainings. (C) Quantification of pTyr front-back ratio (n=14): error bars indicate s.e.m. (D-D″) *sec3*^{GT} mosaic border cell cluster fails to display polarized F-actin staining. (E-E‴) A border cell cluster that is entirely mutant for *sec3*^{GT} (marked by absence of GFP) does not show polarized pTyr staining at the front. F-actin is labeled by rhodamine phalloidin. Scale bar: 5 μm.

drove *Gal4* expression not only in all the migratory border cells (outer border cells, excluding the central nonmigratory polar cells) but also in a subset of centripetal, posterior and a few sporadically positioned follicle cells (Jékely et al., 2005). Interestingly, Rab11-labeled recycling endosome was strongly upregulated in all follicle cells expressing λ-PVR (Fig. 4B-B″,L), consistent with that of the Rab11 staining increase in λ-PVR-expressing border cells (Fig. 3D′; Fig. 4K). Likewise, PVR overexpression caused a milder but still significant increase in a few posterior follicle cells, and the increase in Rab11 staining was proximal to the basal region of follicle epithelium (Fig. 4E,E′). As the overexpressed PVR also had a basal junctional localization (Fig. 4E′) (Jékely et al., 2005), the close proximity between PVR and Rab11 suggests that PVR sends a signal to locally increase the recycling endosome levels. By contrast, stainings for Sec5 and Rab5 (early endosome marker, supplementary material Fig. S3E) were not affected in λ-PVR-expressing follicle cells (Fig. 4C-D′), indicating that PVR specifically affects recycling endosome.

To test whether λ-PVR increases Rab11 expression or promotes only the formation of recycling endosome, we expressed *UAS-Rab11-GFP* in the border cells using *slbo-Gal4*. We found that λ-PVR strongly increased the total levels of Rab11-GFP in border cells and follicle cells (supplementary material Fig. S6), in the same way that it increased endogenous Rab11 stainings. This indicates that the increase in Rab11-GFP levels is unlikely through transcription upregulation by PVR signaling, as the *UAS-Rab11-GFP* is only subject to transcriptional regulation of the yeast Gal4 protein. This result suggests that ectopic PVR signaling does not upregulate the expression level of Rab11, but it promotes the formation of recycling endosomes, which are manifested as strong aggregates or large masses that are labeled by intense Rab11 stainings or strong Rab11-GFP signals (supplementary material Fig. S6B′,D′; Fig. 3D′; Fig. 4B′). This enlargement of Rab11-stained structures is consistent with a recent report, which showed that increase of Rab11 activity resulted in enlargement of Sec15-labeled vesicles in the border cells (Laflamme et al., 2012).

We next sought to identify the downstream signal of PVR that mediates this effect. One candidate is the small GTPase Rac, which had been previously shown to act genetically downstream of PVR to promote actin polymerization and lamellipodial protrusion in both follicle cells and border cells (Duchek et al., 2001). Interestingly, reducing the function of Rac by co-expressing a dominant-negative form of Rac (RacN17) (Geisbrecht and Montell, 2004; Zhang et al., 2011), in the λ-PVR expressing background, dramatically rescued the phenotype and reverted the high levels of Rab11 back to almost wild-type levels and pattern (Fig. 4G-G″,K,L). This rescue is specific and not due to an extra copy of *UAS* transgene, as co-expression of *UAS-lacZ* transgene has no rescuing effect (Fig. 4L). Furthermore, expression of RacN17 alone did not reduce overall

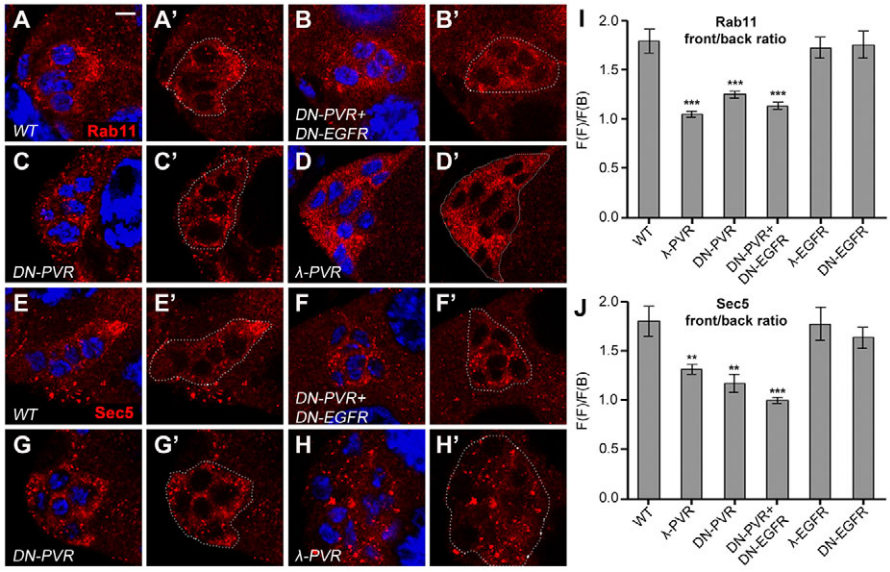

Fig. 3. The asymmetric localization of Rab11 and Sec5 is mediated by RTK signaling. (A-H′) The asymmetric localization of Rab11 and Sec5 near the leading edge, as observed in the wild type (A,A′,E,E′), is abolished in border cells expressing DN-PVR and DN-EGFR (B,B′,F,F′), DN-PVR (C,C′,G,G′), and λ-PVR (D,D′,H,H′). (I,J) Fluorescence intensity was measured for Rab11 (I) and Sec5 (J) for both front and back regions of border cell clusters (genotypes shown on the *x*-axis), and the values were used to calculate the front/back ratios, which are F(Front)/F(Back) and abbreviated as F(F)/F(B). See Materials and methods for details. Error bars indicate s.e.m.; 13<n<16; **P<0.01; ***P<0.001. Scale bar: 5 μm.

Development (2013) doi:10.1242/dev.094979

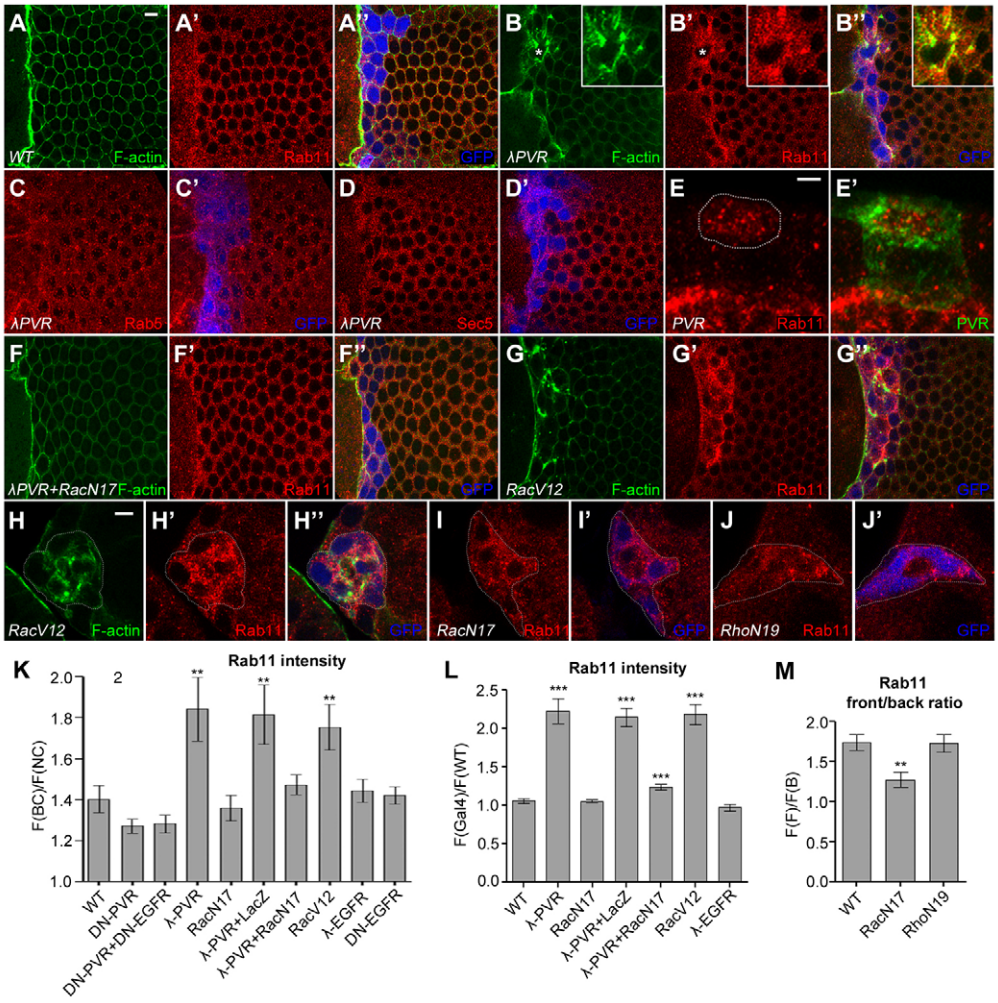

Fig. 4. PVR affects Rab11 levels through Rac. (A-A″) The control follicle cells expressing *UAS-GFP* by *slbo-Gal4* display Rab11 levels that are comparable to adjacent follicles that are not marked by GFP. A strong line of F-actin staining at the left side of (A) separates nurse cells from follicle cells. (B-D′) Expression of λPVR by *slbo-Gal4* in follicle cells (labeled by GFP) strongly increases the Rab11 levels (inset shows an enlargement of the area marked with *), but do not affect the Rab5 (C,C′) and Sec5 (D,D′) levels, compared with the adjacent unaffected cells (not marked by GFP). (E,E′) Upon PVR overexpression, PVR is enriched in the basal membrane of a columnar-shaped follicle epithelial cell; increased Rab11 stainings are also found proximal to the basal region. The 3D view shown is a maximal projection of a *z*-series of 26 confocal images, with each slice taken at a 0.5 μm step. Basal side is up and apical side (facing oocyte) is down. (F-F″) The *RacN17* transgene restores Rab11 and F-actin to almost wild-type levels in λPVR-expressing follicle cells. Images in B,B′ and G,G′ were taken at lower confocal settings than the control (A,A′) to avoid overexposure of the F-actin and Rab11 stainings. (G-H″) Expression of *RacV12* also elevates Rab11 and F-actin levels in both follicle cells (G-G″) and border cells (H-H″). (I,I′) Expression of *RacN17* reduces the asymmetry of Rab11, whereas (J,J′) *RhoN19* expression has no effect. (K) Fluorescence intensity for Rab11 was measured in both border cells [F(BC)] and nurse cells [F(NC)] of each egg chamber, and the values were used to calculate F(BC)/F(NC), which represents the normalized levels for Rab11 fluorescence signals in border cells (13 <*n*<16). See Materials and methods for details. (L) Fluorescence intensity for Rab11 was measured in the *slbo-Gal4*-expressing follicle cells [F(Gal4)] and the adjacent wild-type follicle cells [F(WT)], and the values were used to calculate F(Gal4)/F(WT), which represents the normalized levels for Rab11 in the *slbo-Gal4*-expressing follicle cells (*n*=10). (M) The front/back ratios of Rab11 in border cell clusters were calculated as in Fig. 3I. Error bars indicate s.e.m. ***P*<0.01; ****P*<0.001. Scale bars: in A, 5 μm for A-D′,F-G″; in E, 2 μm for E,E′; in H, 5 μm for H-J′.

levels of Rab11, but significantly reduced its front-back ratio (Fig. 4I,K,M). By contrast, increasing the activity of Rac by expressing a constitutive active form of Rac (RacV12) (Duchek et al., 2001) elevated the levels of Rab11 in border cells and follicle cells (Fig. 4G-H″,K,L). We found that after RacV12 expression or λ-PVR expression, 82% (*n*=94) or 90% (*n*=88) of GFP-labeled follicle cells, respectively, had significantly higher Rab11 levels.

A noted feature from λ-PVR (or RacV12) overexpression in both border cells and follicle cells is the strong increase in actin polymerization, and RacN17 co-expression suppressed both the F-actin and Rab11 staining increases. These data raised a possibility that actin polymerization is directly responsible for the elevated recycling endosome levels in both border cells and follicle cells. To test this idea, we treated wild-type egg chambers with an F-actin destabilizing drug Latrunculin A (Lat-A) to reduce F-actin levels (Zhang et al., 2011). Stage-9 egg chambers incubated with control medium for 1 hour displayed a normal morphology and wild-type phenotype, including F-actin and Rab11 enrichment at the leading edge of border cell cluster (Fig. 5A-A″). Interestingly, incubation with Lat-A (2 μM) containing medium for 1 hour resulted in a loss of front bias of Rab11 staining while causing a dramatic reduction of F-actin levels in border cells (Fig. 5B-B″). Moreover, reducing the actin depolymerizing activity by knocking down the Cofilin (Actin depolymerizing factor; Twinstar – FlyBase) (Zhang et al.,

Development (2013) doi:10.1242/dev.094979

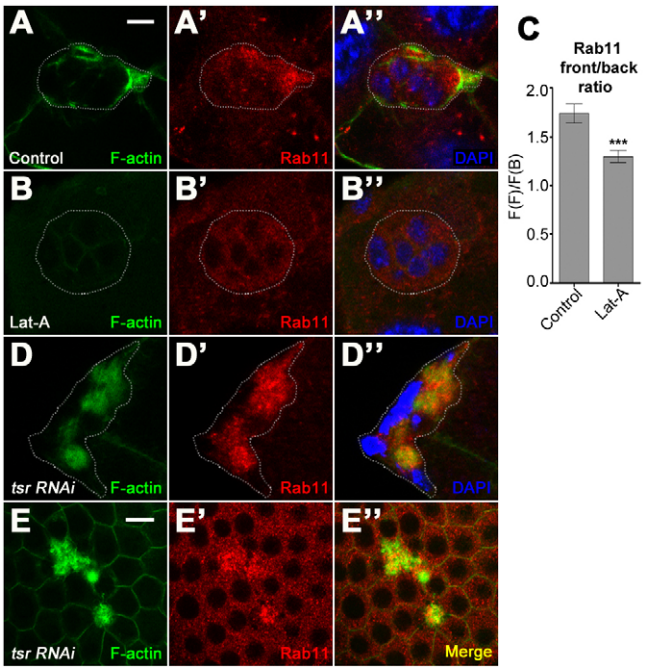

Fig. 5. Manipulation of F-actin levels affects Rab11 levels.
(A-B″) Polarization of both F-actin and Rab11 are abolished in border cells by treatment with the F-actin-depolymerizing drug Lat-A. (C) Quantification of the front/back ratio of Rab11 in control and in Lat-A treated border cell clusters. (D-E″) Ectopic F-actin caused by *tsr* RNAi results in strong increase in the Rab11 levels in both border cells (D-D″) and follicle cells (E-E″). DAPI labels nuclei. Scale bars: 5 μm.

2011) encoding gene *tsr* in the border cells and follicle cells resulted in ectopic strong F-actin regions, which also led to a strong increase in the Rab11 levels (Fig. 5D-E″), further demonstrating that F-actin levels directly affected recycling endosome levels. Interestingly, the elevated Rab11 stainings or Rab11-GFP signals were often proximal to or partially overlapping the strong F-actin stainings. Such a complementary or overlapping pattern was often observed around the leading edge of wild-type border cells (Fig. 5A-A″; supplementary material Fig. S4B and Fig. S6A″), and near the ectopic F-actin regions within the λ-PVR, RacV12 or *tsr* RNAi expressing follicle cells and border cells (Fig. 4B′,G′,H′; Fig. 5D-E″; supplementary material Fig. S6B″,D″). Lastly, we treated the λ-PVR expressing egg chambers with Lat-A for 1 hour but found no significant rescuing effect (data not shown). The difference in results from the RacN17 rescue and the Lat-A treatment is likely to be due to the difference in the rescue timings. RacN17 is expressed at the same time as λ-PVR expression, whereas Lat-A treatment is applied several hours later (than λ-PVR expression), when the strong inducing effect from λ-PVR has been fully manifested and the massive recycling endosome structure cannot be easily reverted back to its normal formation. Taken together, our results showed that PVR signaled through Rac to strongly induce recycling endosome formation in border cells, probably in an F-actin-dependent manner.

Exocyst promotes recycling and tethering of E-cadherin-containing vesicles in follicle cells and border cells

Next, we sought to understand what kinds of cargo are transported by the Rab11-labeled vesicles and what role exocyst plays in regulating transport of these vesicles during border cell migration. Previous studies have shown that the exocyst promotes polarized recycling of epithelial polarity molecules such as E-cadherin onto the plasma membrane of epithelial cells, probably via the vesicle-tethering function of the exocyst (Blankenship et al., 2007; Classen et al., 2005; Langevin et al., 2005). E-cadherin is not only an essential component of the subapically localized adherens junction in follicle epithelium but also a major adhesive molecule required for the adhesion of border cells to the substrate (nurse cells) and for their migration (Niewiadomska et al., 1999). It was previously reported that E-cadherin pattern is disrupted by Rab11 deficiency in border cells (Cobreros-Reguera et al., 2010). To determine whether exocyst regulates recycling of E-cadherin or other epithelial polarity proteins during border cell migration, we carried out a detailed phenotypic analysis of *sec3* mutant border cells. Mosaic border cell clusters containing *sec3* homozygous mutant clones showed that cytoplasmic dots of E-cadherin staining appeared enlarged and irregularly shaped compared with the wild-type border cells and were strongly elevated in levels in 15% of mutant clones examined (60 mosaic clusters examined; Fig. 6A-B″). A high proportion of these enlarged and irregular structures either colocalized or overlapped with Rab11-labeled structures, which were also strongly upregulated and appeared enlarged and irregular as compared to the wild type (Fig. 6A-B″). By contrast, none of the *sec3* mutant clones displayed significant increase or disruption in stainings for Baz/Par-3 (n=48; Fig. 6D,D′) and Dlg1 (n=45; Fig. 6E,E′), which are polarity molecules associated with apical and lateral junctions, respectively, and are involved in regulation of border cell migration (Goode and Perrimon, 1997; Pinheiro and Montell, 2004; Szafranski and Goode, 2004). Furthermore, *sec15* mutant border cells displayed a similar phenotype to that of the *sec3* mutant (supplementary material Fig. S7A-A″). Likewise, follicle epithelium containing *sec3* or *sec15* mutant clones also exhibited a dramatic simultaneous increase in both E-cadherin and Rab11 stainings at the subapical cytoplasmic region (15 of 84 *sec3* clones, Fig. 6C-C″; 12 of 30 *sec15* clones examined, supplementary material Fig. S7B-B″). Upon closer examination, the colocalization pattern between the two highly elevated stainings varies from almost total colocalization (supplementary material Fig. S7B-B″,D-D″) to strong overlap (Fig. 6C-C″). Consistent with the border cell data, the distribution pattern and amount of Baz/Par-3 (n=62) and Dlg1 (n=57) were not affected in the *sec3* mutant follicle cells (Fig. 6F-G′). To determine whether the colocalization of E-cadherin is specific only to recycling endosome and not to other compartments, Golgi, early endosome and late endosome were stained with Lva (Lava lamp), Rab5 and Hrs, respectively. We found no significant colocalization between the highly elevated E-cadherin staining and Lva, Rab5 or Hrs staining (supplementary material Fig. S8; data not shown). Together, the above data show that E-cadherin is a specific cargo transported by the recycling endosome in border cells and follicle cells.

Lastly, we tested whether Sec3 promoted the tethering and delivery of E-cadherin-containing vesicles onto the plasma membrane, as expected for a functional component of the exocyst complex. We utilized a previously reported assay (Langevin et al., 2005) that detected only the membrane-bound E-cadherin but not the intracellular E-cadherin pool in the follicle epithelium. Stage-9 or -10 egg chambers were incubated with the DCAD2 antibody that detects an epitope in the extracellular region of E-cadherin, and the incubation was performed at 4°C for 30 minutes to prevent endocytosis of the antibody. After incubation, fixing (cell permeabilization) and staining with a secondary antibody would allow visualization of the pool of E-cadherin delivered onto the lateral membrane only. Indeed, within a $sec3^{GT}$ mosaic follicle epithelium, *sec3* mutant follicle cells displayed a significant decrease of membrane E-cadherin staining compared with the

Development (2013) doi:10.1242/dev.094979

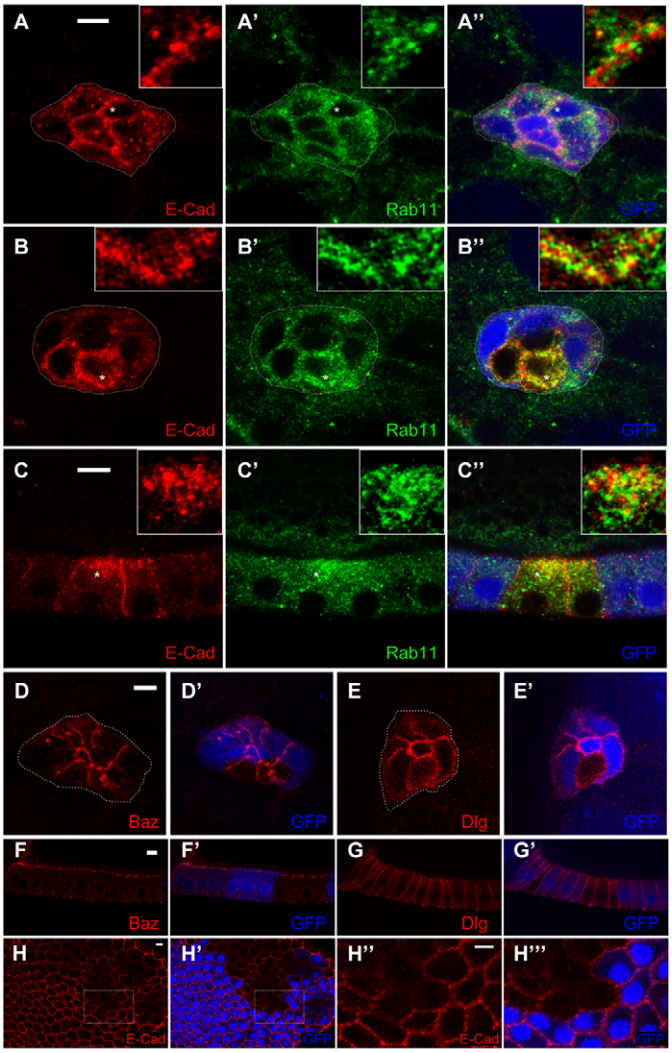

Fig. 6. Loss of Sec3 function blocks recycling and delivery of E-cadherin-containing vesicles to the membrane. (A-E′) E-cadherin (B-B″), but not Baz (D,D′) or Dlg1 (E,E′) accumulates in Rab11-marked vesicles in *sec3* mutant border cells (marked by lack of GFP), compared to the wild-type control (A-A″). (A-C″) An enlarged view of the area marked with * is shown in the insets. The insets in A-A″ show occasional colocalization of two spots stained for E-cadherin and Rab11. E-cadherin (C-C″), but not Baz (F,F′) or Dlg1 (G,G′) accumulates in Rab11-labeled vesicles in *sec3* mutant follicle cells (marked by lack of GFP). (H-H‴) An assay detects only a membrane-bound pool of E-cadherin; see Materials and methods for details. *sec3* mutant follicle cells display less membrane-bound E-cadherin in the lateral membrane than the adjacent wild-type cells. Scale bars: 5 μm.

adjacent wild-type cells (Fig. 6H-H‴). Taken together, these results indicated that exocyst promoted the tethering and delivery of E-cadherin-containing vesicles onto the plasma membrane and the deficiency of exocyst function probably blocked such delivery and caused an accumulation and enlargement of Rab11-labeled recycling endosomes, which contained E-cadherin as a specific cargo during both border cell migration and follicle cell morphogenesis.

DISCUSSION

It has been proposed that repeated cycles of endocytosis of RTKs (or active RTKs) and recycling of them back to the membrane would effectively concentrate active RTK in the front of the migrating border cells (Assaker et al., 2010; Jékely et al., 2005; Montell et al., 2012). However, if the levels of endocytic recycling remain uniform in all the outer border cells during migration, a fast amplification of RTK activity levels between front and back would be difficult to achieve. Here, we show that there is a polarized endogenous distribution of the recycling endosome and exocyst in the leading border cells within the migrating cluster, which could conceivably make such amplification faster and more efficient in the leading cells. It was also shown previously that Sec15-GFP has an asymmetric localization at the front, when it is overexpressed in border cells (Assaker et al., 2010). Along their migrating route, the border cells often tumble or rotate as a cluster, resulting in position changes such as front cells becoming lateral and back cells and vice versa (Bianco et al., 2007). In such a scenario, a fast and robust amplification process would be essential to relocalize active RTKs. Indeed, we found that overexpressing Sec3 or Rab11-GFP, but not Sec5-GFP (Kakihara et al., 2008), in a single cell clone within a mosaic border cell cluster significantly promoted the likelihood of such a cell being positioned at the leading position (supplementary material Fig. S2), suggesting that this cell utilizes its increased recycling and tethering to amplify and relocalize active RTKs faster and more efficiently than other wild-type neighbor cells. The difference in promoting effect from Sec3 and Sec5 is interesting, suggesting that when overexpressed the Sec3 subunit is more able to enhance the overall exocyst function than Sec5. This is consistent with a Sec3 study in budding yeast, which shows that as a unique subunit of exocyst Sec3 serves as a spatial landmark on the bud tip to recruit a subcomplex (comprising seven subunits) of exocyst containing all subunits but Sec3 (Boyd et al., 2004; Finger et al., 1998). Only when the subcomplex along with the associated vesicle arrives at the bud tip, can Sec3 be joined with it to form a fully functional tethering complex.

The next question is how the polarized distribution of recycling and tethering activity is initiated in border cells. We demonstrated that this was likely to be induced by the guidance receptors in response to the external gradient of guidance cues, as removing guidance signaling by DN-PVR and DN-EGFR expression abolished Rab11 and Sec5 polarized distribution, and DN-PVR expression alone markedly reduced the polarization. These data suggested the presence of a positive feedback loop of active RTKs–endocytic recycling–active RTKs in border cells, as Rab11 and exocyst components (Sec3 and Sec15) were shown to be conversely required for polarized pTyr or active RTK localization at the front (this study; Assaker et al., 2010; Janssens et al., 2010). Interestingly, we find PVR signals downstream through Rac and then polymerized actin to promote recycling endosome levels, providing mechanistic details to this feedback loop (Fig. 7). Interestingly, it was recently shown that Rab11 interacts with Rac and actin cytoskeleton regulator moesin during border cell migration (Ramel et al., 2013). Furthermore, we found that strong Rab11 stainings were proximal to or partially overlapping with strong F-actin staining in the leading edge of wild-type border cells and around the ectopic F-actin regions in the λ-PVR, RacV12 or *tsr*-RNAi expressing follicle cells and border cells. F-actin appears to be the direct cause rather than the effect of recycling endosome accumulation, because manipulating its levels by Lat-A or *tsr* RNAi leads to either up- or downregulation of the levels of recycling endosome. However, we cannot rule out the possibility that Rac can somehow act on recycling endosome-associated regulators directly (independently of F-actin) to affect their function. It was previously shown that actin polymerization is required for recycling of cargo back to plasma membrane, possibly through F-actin serving as a track for the movement of vesicles (Grant and Donaldson, 2009;

Development (2013) doi:10.1242/dev.094979

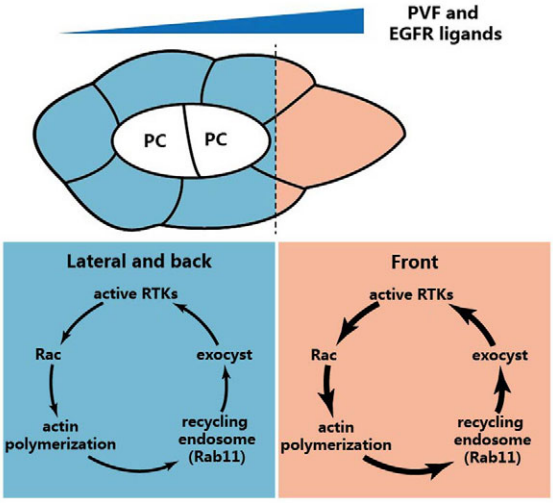

Fig. 7. A model showing a positive-feedback loop promoting guided collective migration of border cells. As shown in the diagram, each outer border cell [excluding the polar cells (PC)] within the cluster has an intrinsic feedback loop as described in the Discussion. But the cell(s) in the front respond to an external gradient of guidance cues and produce a moderately higher RTK signaling than in the cells positioned in the lateral and back region. The positive feedback loop is able to amplify the moderate difference in RTK activity levels between front and back border cells presumably over a short period of time, resulting in a highly polarized enrichment of active RTK in the front, which guides the collective cell migration of border cells toward the oocyte.

Radhakrishna and Donaldson, 1997; Weigert et al., 2004). However, how F-actin induces recycling endosome formation and organization is not clear and remains to be elucidated.

It was previously proposed that recycling of active RTKs needs to be directional (toward the front) to achieve polarized RTK activity (Janssens et al., 2010; Jékely et al., 2005; Montell et al., 2012). If active RTKs in the leading edge are endocytosed and then recycled to new regions in the membrane, RTK activity would be delocalized. What causes the recycling to be directed toward the front membrane is not clear. Our proposed feedback loop via F-actin suggests that the active PVR (RTK) in the leading edge could locally induce higher levels of recycling endosome through Rac and enhanced actin polymerization (by Rac). As a result, the directional recycling could be achieved with the localized actin filaments serving both as a recycling endosome inducing agent and as tracks for movement of vesicles (carrying active RTKs) toward the front membrane, which prevents the active RTKs from being recycled to elsewhere and becoming delocalized. Indeed, inhibiting actin polymerization in the border cells by Lat-A treatment abolished both the polarized F-actin and the elevated Rab11 stainings proximal to F-actin, which are normally present in the leading edge of the wild-type cluster.

Lastly, our work also provides some insight into the kinds of cargo that are recycled during border cell migration. We show that E-cadherin is a specific cargo. E-cadherin is the major adhesion molecule required for border cell migration (Niewiadomska et al., 1999), whereas integrin plays only a minor role and is not required in border cells (Devenport and Brown, 2004; Dinkins et al., 2008). Our finding suggests that cycles of endocytosis and recycling of E-cadherin could promote the dynamic assembly and disassembly of E-cadherin-mediated adhesion on the substrate (nurse cell E-cadherin), similar to how the turnover of integrin at the focal adhesion is regulated by endocytic recycling in mammalian cells (Caswell and Norman, 2008; Caswell et al., 2007; Ulrich and Heisenberg, 2009). Interestingly, we often observed that elevated intracellular E-cad stainings tend to be localized below the cell membrane that juxtaposes nurse cell membrane (supplementary material Fig. S7A,C), suggesting that E-cadherin is normally delivered to or recycled back to this membrane region by Rab11 and exocyst during adhesion and migration. Another important candidate cargo to be determined is PVR. However, we have been unable to detect significant colocalization between Rab11 with PVR or active PVR with the previously reported PVR or pPVR antibody (Janssens et al., 2010; Jékely et al., 2005). Therefore, the definitive role of PVR or active PVR as a cargo for recycling still awaits further determination.

MATERIALS AND METHODS

Drosophila genetics

Flies were cultured following standard procedures at 25°C except for RNAi experiments at 29°C. All strains were obtained from the Bloomington *Drosophila* Stock Center, except for the following: $sec3^{GT}$*/TM6B* (Chen et al., 2005), $Rab11^{j2D1}$, $Rab5^{k08232}$, $sec3^{PBac}$*/TM6B* (Drosophila Genetic Resource Center), *UAS-sec5-GFP* (Hayashi's lab), *sec3* RNAi (Vienna *Drosophila* RNAi Center), *UAS-DNPVR/Cyo* (Montell's lab), *UAS-DNPVR, UAS-DNEGFR/Cyo, UAS-λPVR/TM3* (Rørth's lab). To generate *UAS-sec3* transgenic line, a full-length cDNA of the *sec3* gene was subcloned into a modified pUAST-attB vector and was injected into embryos according to standard procedures. Mutant *FRT* clones were induced using *hs-FLP*. Flies were heat shocked for 1 hour per day at 37°C for 3 days before eclosion and 1 day after eclosion, then dissected 2-3 days after the last heat shock. To perform flip-out experiments, *AyGAL4 UAS-GFP* (or *UAS-sec3*, or *UAS-rab11-GFP*, or *UAS-sec5-GFP*) was crossed to *hs-Flp*. Newly eclosed flies were heat shocked at 37°C for 4.5 minutes, and dissected after 2-3 days. Only mosaic border cell clusters with one-cell flip-out clone were used for analysis.

Immunohistochemistry and microscopy

Ovary dissection was carried out in PBS and then fixed in devitellinizing buffer (7% formaldehyde) and heptane (Sigma) mixture (1:6) for 10 minutes. After washes in PBS, ovaries were incubated in blocking solution (PBT, 10% goat serum) for 30 minutes and then stained overnight at 4°C. Note that we and some labs used the formaldehyde/heptanes method for fixing egg chambers, whereas other labs used formaldehyde only method, which may result in variability in staining patterns. But, we have used both methods for E-cadherin staining and found both produced similar staining patterns (data not shown). Primary antibodies and their concentrations were as follows: mouse anti-phospho-Tyr (1:200, 4G10, Millipore), mouse anti-Rab11 (1:200, BD Transduction), rat anti-E-Cad (DCAD2, 1:50, DSHB), rabbit anti-Baz (1:400, gift from A. Wodarz), mouse anti-Dlg1 (1:100, DSHB), mouse anti-Sec5 (1:50, gift from T. Schwarz), Rabbit anti-Rab5 (1:200, Abcam) and rat anti-PVR (1:200, gift from P. Rørth). After washes in PBT, ovaries were incubated with secondary antibodies (Jackson ImmunoResearch) for 2 hours at room temperature. F-actin was labeled by Rhodamine phalloidin (1:100, Sigma). Confocal images were obtained using a Leica TCS SP5 II (with HyD detector) or an Olympus FV1000 confocal microscope.

Quantification of fluorescence signals

The quantification methods are similar to that described previously (Zhang et al., 2011). For measurement of the front/back ratios, an area around the leading edge of the cluster, but excluding polar cells (labeled by lack of GFP from *slbo-Gal4*), was chosen as the front region, and an area including the lagging end and excluding polar cells was chosen as the back region. Fluorescence intensity (FI) and area were measured in ImageJ software (NIH) for each region; the front/back ratios were calculated as [front FI/front area] divided by [back FI/back area]. For measurement of Rab11's levels in the *slbo-Gal4:UAS-GFP* marked border cells and follicle cells, nurse cells or follicle cells (not marked by GFP) adjacent to the GFP-marked border cells or follicles respectively are used for normalization of fluorescence,

because their constant and uniform levels of Rab11 staining are not affected by *slbo-Gal4:UAS-transgene*. FI and area were measured in ImageJ for each area as mentioned above and were used for the following calculations: normalized Rab11 levels in border cells=[border cells FI/border cells area] divided by [nurse cells FI/nurse cells area]; normalized Rab11 levels in Gal4 expressing follicle cells=[Gal4 FCs FI/Gal4 FCs area] divided by [adjacent WT FCs FI/adjacent WT FCs area].

Latrunculin A treatment

Ovaries were dissected and cultured in Schneider's medium cocktail as described previously for use of live imaging (Chu et al., 2012; Prasad and Montell, 2007). After dissection, egg chambers were incubated in Latrunculin A (2 μM in Schneider's medium cocktail, Invitrogen) for 1 hour before fixation, and were then stained as described above.

Antibody binding assay on dissected egg chamber

Egg chambers were incubated with the anti-DE-Cadherin (DCAD2 diluted at 1:10) antibody in the Schneider's medium cocktail for 30 minutes at 4°C. Following three washes in Schneider's medium at 4°C, egg chambers were fixed and then stained as described above, the procedure is similar to that previously described (Langevin et al., 2005).

Acknowledgements

We thank Bloomington *Drosophila* Stock Center, *Drosophila* Genetic Resource Center, Vienna *Drosophila* RNAi Center, Pernile Rørth, Denise Montell and Shigeo Hayashi for fly stocks; and Thomas Schwarz, Andreas Wodarz and Pernile Rørth for antibody reagents.

Competing interests

The authors declare no competing financial interests.

Author contributions

J.C. and P.W. conceived and designed the experiments; P.W. and D.W. collected and analyzed the data; J.C. and P.W. prepared the manuscript; J.L., D.C., H.W. and L.Z. performed important preliminary experiments supporting this study; J.L. prepared one of the figures.

Funding

This work is supported by grants from National Natural Sciences Foundation of China [31171335, 31271488, 31071219 to J.C.].

Supplementary material

Supplementary material available online at
http://dev.biologists.org/lookup/suppl/doi:10.1242/dev.094979/-/DC1

References

Alone, D. P., Tiwari, A. K., Mandal, L., Li, M., Mechler, B. M. and Roy, J. K. (2005). Rab11 is required during Drosophila eye development. *Int. J. Dev. Biol.* **49**, 873-879.

Assaker, G., Ramel, D., Wculek, S. K., González-Gaitán, M. and Emery, G. (2010). Spatial restriction of receptor tyrosine kinase activity through a polarized endocytic cycle controls border cell migration. *Proc. Natl. Acad. Sci. USA* **107**, 22558-22563.

Beronja, S., Laprise, P., Papoulas, O., Pellikka, M., Sisson, J. and Tepass, U. (2005). Essential function of Drosophila Sec6 in apical exocytosis of epithelial photoreceptor cells. *J. Cell Biol.* **169**, 635-646.

Bianco, A., Poukkula, M., Cliffe, A., Mathieu, J., Luque, C. M., Fulga, T. A. and Rørth, P. (2007). Two distinct modes of guidance signalling during collective migration of border cells. *Nature* **448**, 362-365.

Blankenship, J. T., Fuller, M. T. and Zallen, J. A. (2007). The Drosophila homolog of the Exo84 exocyst subunit promotes apical epithelial identity. *J. Cell Sci.* **120**, 3099-3110.

Boyd, C., Hughes, T., Pypaert, M. and Novick, P. (2004). Vesicles carry most exocyst subunits to exocytic sites marked by the remaining two subunits, Sec3p and Exo70p. *J. Cell Biol.* **167**, 889-901.

Caswell, P. and Norman, J. (2008). Endocytic transport of integrins during cell migration and invasion. *Trends Cell Biol.* **18**, 257-263.

Caswell, P. T., Spence, H. J., Parsons, M., White, D. P., Clark, K., Cheng, K. W., Mills, G. B., Humphries, M. J., Messent, A. J., Anderson, K. I. et al. (2007). Rab25 associates with alpha5beta1 integrin to promote invasive migration in 3D microenvironments. *Dev. Cell* **13**, 496-510.

Chen, J., Call, G. B., Beyer, E., Bui, C., Cespedes, A., Chan, A., Chan, J., Chan, S., Chhabra, A., Dang, P. et al. (2005). Discovery-based science education: functional genomic dissection in Drosophila by undergraduate researchers. *PLoS Biol.* **3**, e59.

Chu, D., Pan, H., Wan, P., Wu, J., Luo, J., Zhu, H. and Chen, J. (2012). AIP1 acts with cofilin to control actin dynamics during epithelial morphogenesis. *Development* **139**, 3561-3571.

Classen, A. K., Anderson, K. I., Marois, E. and Eaton, S. (2005). Hexagonal packing of Drosophila wing epithelial cells by the planar cell polarity pathway. *Dev. Cell* **9**, 805-817.

Cobreros-Reguera, L., Fernández-Miñán, A., Fernández-Espartero, C. H., López-Schier, H., González-Reyes, A. and Martín-Bermudo, M. D. (2010). The Ste20 kinase misshapen is essential for the invasive behaviour of ovarian epithelial cells in Drosophila. *EMBO Rep.* **11**, 943-949.

Devenport, D. and Brown, N. H. (2004). Morphogenesis in the absence of integrins: mutation of both Drosophila beta subunits prevents midgut migration. *Development* **131**, 5405-5415.

Devreotes, P. and Janetopoulos, C. (2003). Eukaryotic chemotaxis: distinctions between directional sensing and polarization. *J. Biol. Chem.* **278**, 20445-20448.

Dinkins, M. B., Fratto, V. M. and Lemosy, E. K. (2008). Integrin alpha chains exhibit distinct temporal and spatial localization patterns in epithelial cells of the Drosophila ovary. *Dev. Dyn.* **237**, 3927-3939.

Dollar, G., Struckhoff, E., Michaud, J. and Cohen, R. S. (2002). Rab11 polarization of the Drosophila oocyte: a novel link between membrane trafficking, microtubule organization, and oskar mRNA localization and translation. *Development* **129**, 517-526.

Duchek, P., Somogyi, K., Jékely, G., Beccari, S. and Rørth, P. (2001). Guidance of cell migration by the Drosophila PDGF/VEGF receptor. *Cell* **107**, 17-26.

Finger, F. P., Hughes, T. E. and Novick, P. (1998). Sec3p is a spatial landmark for polarized secretion in budding yeast. *Cell* **92**, 559-571.

Friedl, P. and Gilmour, D. (2009). Collective cell migration in morphogenesis, regeneration and cancer. *Nat. Rev. Mol. Cell Biol.* **10**, 445-457.

Geisbrecht, E. R. and Montell, D. J. (2004). A role for Drosophila IAP1-mediated caspase inhibition in Rac-dependent cell migration. *Cell* **118**, 111-125.

Goode, S. and Perrimon, N. (1997). Inhibition of patterned cell shape change and cell invasion by Discs large during Drosophila oogenesis. *Genes Dev.* **11**, 2532-2544.

Grant, B. D. and Donaldson, J. G. (2009). Pathways and mechanisms of endocytic recycling. *Nat. Rev. Mol. Cell Biol.* **10**, 597-608.

He, B. and Guo, W. (2009). The exocyst complex in polarized exocytosis. *Curr. Opin. Cell Biol.* **21**, 537-542.

Jafar-Nejad, H., Andrews, H. K., Acar, M., Bayat, V., Wirtz-Peitz, F., Mehta, S. Q., Knoblich, J. A. and Bellen, H. J. (2005). Sec15, a component of the exocyst, promotes notch signaling during the asymmetric division of Drosophila sensory organ precursors. *Dev. Cell* **9**, 351-363.

Jankovics, F., Sinka, R. and Erdelyi, M. (2001). An interaction type of genetic screen reveals a role of the Rab11 gene in oskar mRNA localization in the developing Drosophila melanogaster oocyte. *Genetics* **158**, 1177-1188.

Janssens, K., Sung, H. H. and Rørth, P. (2010). Direct detection of guidance receptor activity during border cell migration. *Proc. Natl. Acad. Sci. USA* **107**, 7323-7328.

Jékely, G., Sung, H. H., Luque, C. M. and Rørth, P. (2005). Regulators of endocytosis maintain localized receptor tyrosine kinase signaling in guided migration. *Dev. Cell* **9**, 197-207.

Kakihara, K., Shinmyozu, K., Kato, K., Wada, H. and Hayashi, S. (2008). Conversion of plasma membrane topology during epithelial tube connection requires Arf-like 3 small GTPase in Drosophila. *Mech. Dev.* **125**, 325-336.

Laflamme, C., Assaker, G., Ramel, D., Dorn, J. F., She, D., Maddox, P. S. and Emery, G. (2012). Evi5 promotes collective cell migration through its Rab-GAP activity. *J. Cell Biol.* **198**, 57-67.

Langevin, J., Morgan, M. J., Sibarita, J. B., Aresta, S., Murthy, M., Schwarz, T., Camonis, J. and Bellaïche, Y. (2005). Drosophila exocyst components Sec5, Sec6, and Sec15 regulate DE-Cadherin trafficking from recycling endosomes to the plasma membrane. *Dev. Cell* **9**, 365-376.

Maxfield, F. R. and McGraw, T. E. (2004). Endocytic recycling. *Nat. Rev. Mol. Cell Biol.* **5**, 121-132.

Montell, D. J., Yoon, W. H. and Starz-Gaiano, M. (2012). Group choreography: mechanisms orchestrating the collective movement of border cells. *Nat. Rev. Mol. Cell Biol.* **13**, 631-645.

Murthy, M., Garza, D., Scheller, R. H. and Schwarz, T. L. (2003). Mutations in the exocyst component Sec5 disrupt neuronal membrane traffic, but neurotransmitter release persists. *Neuron* **37**, 433-447.

Murthy, M., Teodoro, R. O., Miller, T. P. and Schwarz, T. L. (2010). Sec5, a member of the exocyst complex, mediates Drosophila embryo cellularization. *Development* **137**, 2773-2783.

Niewiadomska, P., Godt, D. and Tepass, U. (1999). DE-Cadherin is required for intercellular motility during Drosophila oogenesis. *J. Cell Biol.* **144**, 533-547.

Pinheiro, E. M. and Montell, D. J. (2004). Requirement for Par-6 and Bazooka in Drosophila border cell migration. *Development* **131**, 5243-5251.

Prasad, M. and Montell, D. J. (2007). Cellular and molecular mechanisms of border cell migration analyzed using time-lapse live-cell imaging. *Dev. Cell* **12**, 997-1005.

Queenan, A. M., Ghabrial, A. and Schüpbach, T. (1997). Ectopic activation of torpedo/Egfr, a Drosophila receptor tyrosine kinase, dorsalizes both the eggshell and the embryo. *Development* **124**, 3871-3880.

Radhakrishna, H. and Donaldson, J. G. (1997). ADP-ribosylation factor 6 regulates a novel plasma membrane recycling pathway. *J. Cell Biol.* **139**, 49-61.

Ramel, D., Wang, X., Laflamme, C., Montell, D. J. and Emery, G. (2013). Rab11 regulates cell-cell communication during collective cell movements. *Nat. Cell Biol.* **15**, 317-324.

Rørth, P. (2011). Whence directionality: guidance mechanisms in solitary and collective cell migration. *Dev. Cell* **20**, 9-18.

Szafranski, P. and Goode, S. (2004). A Fasciclin 2 morphogenetic switch organizes epithelial cell cluster polarity and motility. *Development* **131**, 2023-2036.
Ulrich, F. and Heisenberg, C. P. (2009). Trafficking and cell migration. *Traffic* **10**, 811-818.
Weigert, R., Yeung, A. C., Li, J. and Donaldson, J. G. (2004). Rab22a regulates the recycling of membrane proteins internalized independently of clathrin. *Mol. Biol. Cell* **15**, 3758-3770.
Wu, S., Mehta, S. Q., Pichaud, F., Bellen, H. J. and Quiocho, F. A. (2005). Sec15 interacts with Rab11 via a novel domain and affects Rab11 localization in vivo. *Nat. Struct. Mol. Biol.* **12**, 879-885.
Wucherpfennig, T., Wilsch-Brauninger, M. and Gonzalez-Gaitan, M. (2003). Role of Drosophila Rab5 during endosomal trafficking at the synapse and evoked neurotransmitter release. *J. Cell Biol.* **161**, 609-624.
Zhang, X. M., Ellis, S., Sriratana, A., Mitchell, C. A. and Rowe, T. (2004). Sec15 is an effector for the Rab11 GTPase in mammalian cells. *J. Biol. Chem.* **279**, 43027-43034.
Zhang, L., Luo, J., Wan, P., Wu, J., Laski, F. and Chen, J. (2011). Regulation of cofilin phosphorylation and asymmetry in collective cell migration during morphogenesis. *Development* **138**, 455-464.

Table S1. Rescue of the lethality of *sec3* mutants by wild-type *sec3* transgene

Experiment	Actin-GAL4/Cyo; $sec3^{GT}$/TM6B,Tb X UAS-sec3/Cyo; $sec3^{GT}$/TM6B,Tb	Actin-GAL4/Cyo; $sec3^{PBac}$/TM6B,Tb X UAS-sec3/Cyo; $sec3^{PBac}$/TM6B,Tb
Number of total progeny	182	169
Number of homozygous mutant progeny	6	24
Rescue efficiency	23%	100%

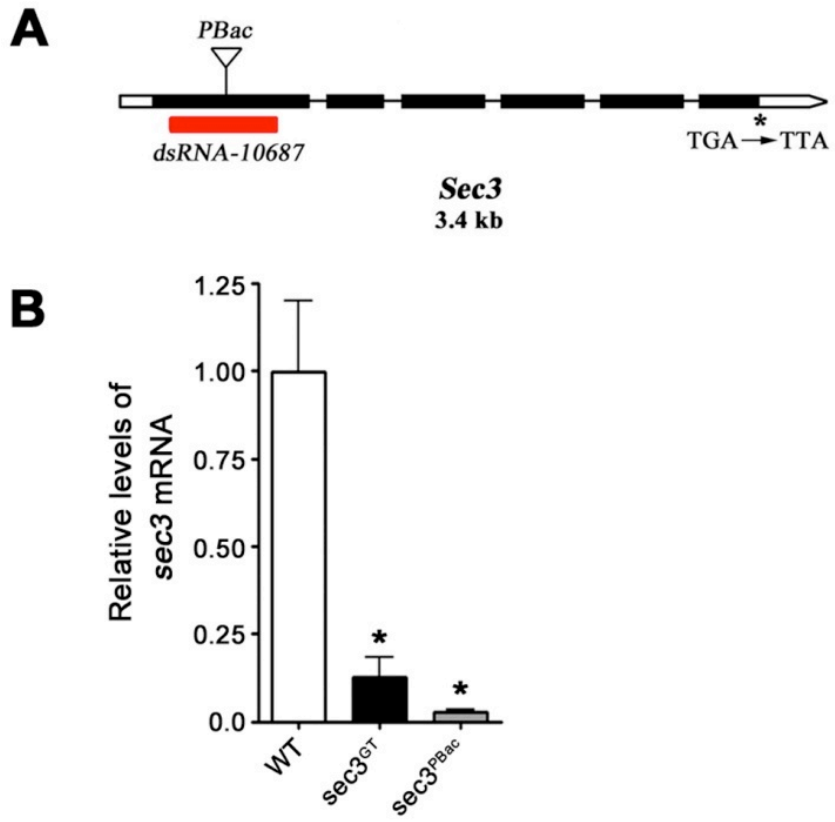

Figure S1. Characterization of the *sec3* mutations. (A), Gene structure and mutant alleles of *sec3*. Black boxes represent the CDS, and white boxes represent untranslated regions. The red box represents the target sequence region of RNAi. $sec3^{PBac}$ is a mutation with *piggyBac* transposon inserted in the first exon of the gene. $sec3^{GT}$ is a point mutation in stop codon. (B), The RNA levels of *sec3* is reduced in *sec3* mutants compared with the wild type flies. Experiments were repeated independently three times with consistent results and three replicates were used per time point.

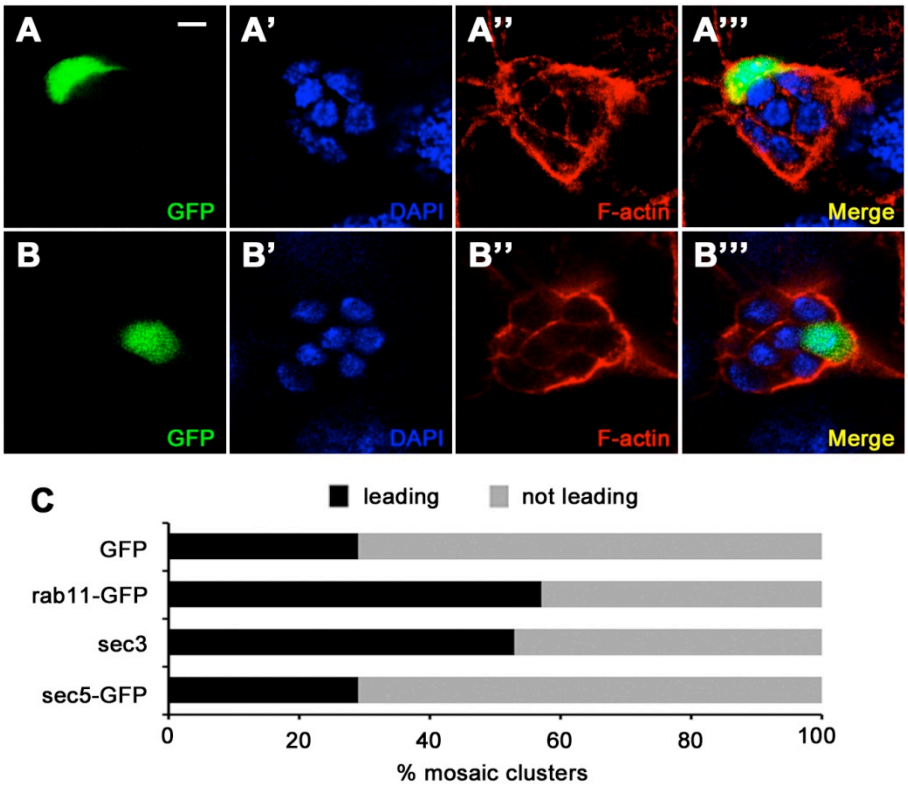

Figure S2. Local increase in Sec3 or Rab11-GFP level in single border cell (BC) biases it to become leading cell for BC cluster. (A-A''') An example of mosaic clusters containing 1-cell clone expressing UAS-*GFP* at the non-leading position. (B-B''') An example of mosaic clusters containing 1-cell clone expressing *UAS-sec3* at the leading position. (C) Cells in clones expressing only the GFP marker became leading cells in 29% of mosaic clusters (n=100), whereas cells expressing Sec3 and Rab11-GFP lead in 53% (n=45) and 57% (n=76) of mosaic clusters, respectively. Expressing Sec5-GFP does not change the frequency of BC becoming leading cell (n=51). Sale bar: 5um.

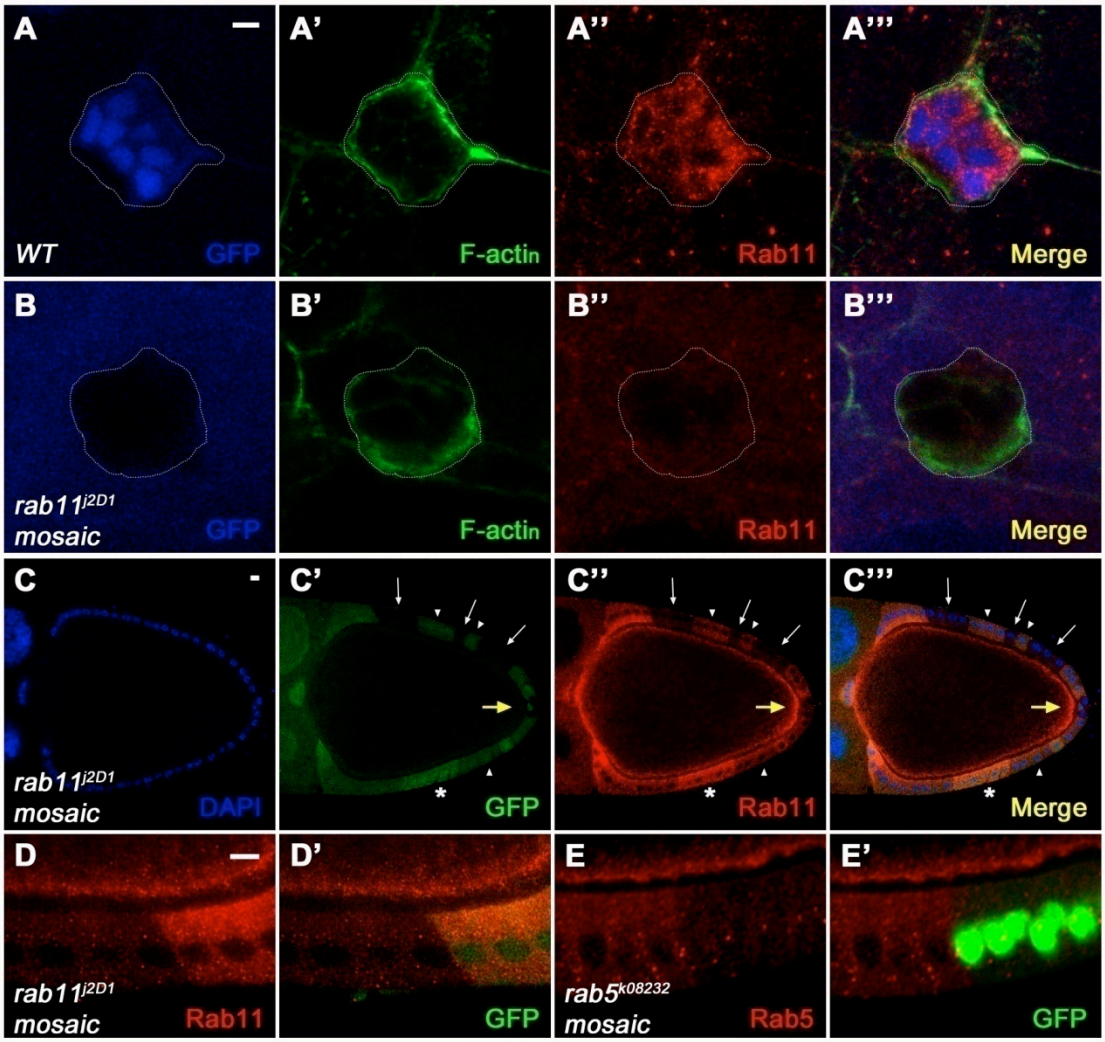

Figure S3. The specificity of Rab11 and Rab5 antibodies. (A-A''') The Rab11 staining in wild type BCs. (B-B''') Rab11 signal is strongly reduced in *rab11*^{j2D1}(Jankovics et al., 2001; Alone et al., 2005) BCs. Mutant cells are marked by absence of GFP. (C-C''') Rab11 signal is strongly reduced in *rab11*^{j2D1} follicle cells (FCs). White arrow shows homozygous mutant cells, arrowhead shows heterozygous cells, * shows wild type cells. Yellow arrow shows specific accumulation of Rab11 at the posterior pole of oocyte as previously reported (Dollar et al., 2002). (D-D'), High magnification view of Rab11 staining in one of the mutant clones shown in (C-C'''). (E-E') Rab5 signal is markedly reduced in a *rab5*^{k08232}(Wucherpfennig et al., 2003) FC clone. Mutant cells are positively marked by GFP. Sale bar: 5um.

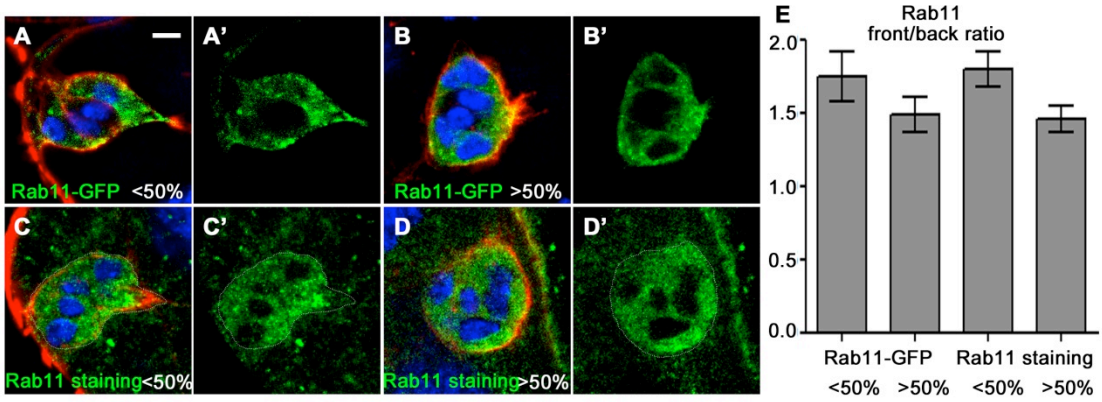

Figure S4. Rab11-GFP is polarized during border cell migration. (A-B'), Representative images showing the distribution of Rab11-GFP at 0%-50% and 50%-100% of the migration process respectively. Blue shows DAPI, red shows F-actin. (C-D') Representative images showing the distribution of Rab11 antibody staining signal at 0%-50% and 50%-100% of the migration process. (E) Fluorescence intensity was measured for Rab11-GFP or Rab11 antibody staining signals in both front[F(F)] and back[F(B)] regions of BC clusters, and the values were used to calculate the F(F)/F(B) ratios (8<n<16). Error bars indicate s.e.m. Scale bar: 5um.

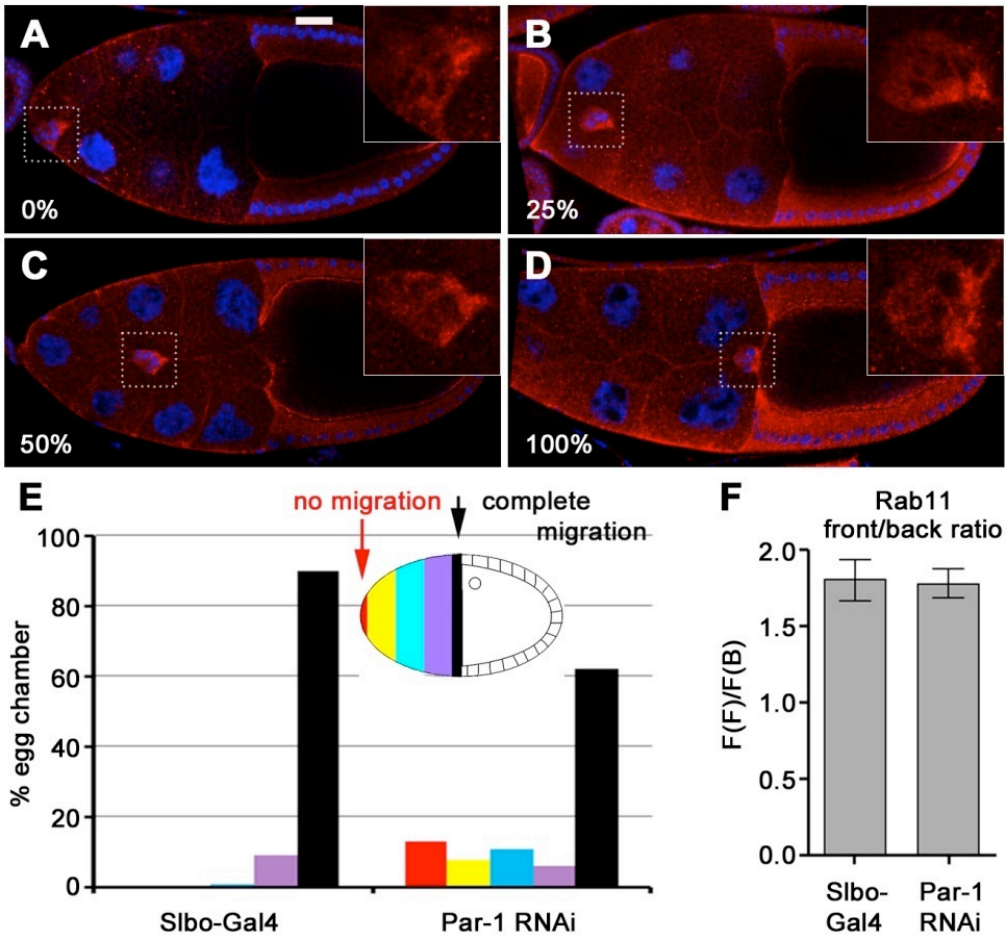

Figure S5. Expression of Par-1 RNAi delays BC migration but does not affect Rab11 polarity. (A-D) Representative images of BC clusters with migration defects or with normal migration all show Rab11 polarity. (E) Quantification of BC migration defects in control or in egg chambers expressing *Par-1 RNAi* driven by *Slbo*-GAL4 (n>80). (F) Quantification of Rab11 front/back ratio. Error bars indicate s.e.m. Scale bar: 20um.

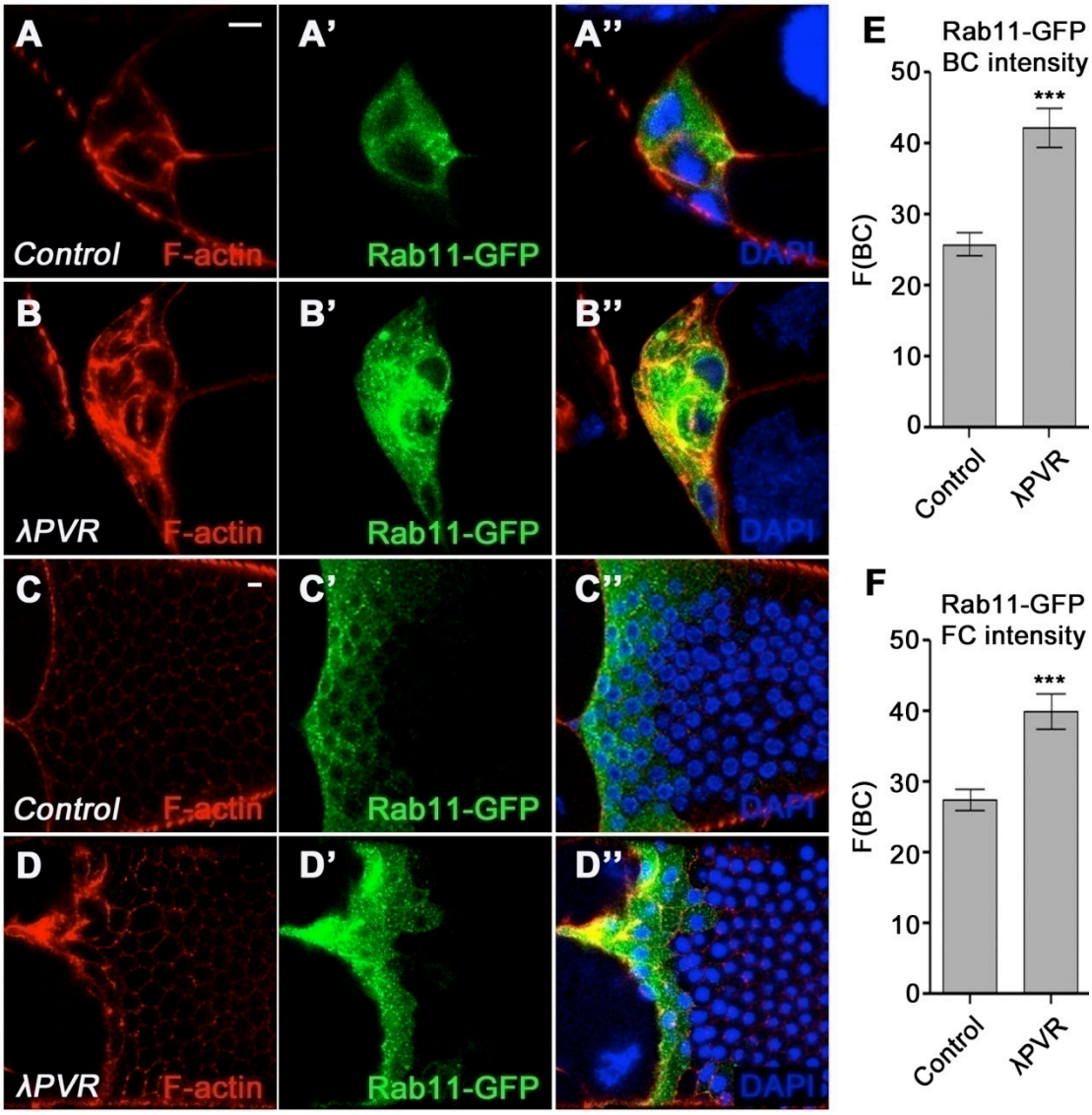

Figure S6. Rab11-GFP intensity is increased in BCs and FCs expressing λPVR. (A-B'',E) Expressing λPVR by Slbo-Gal4 increased Rab11-GFP intensity in BCs. (C-D'',F) Expressing λPVR by Slbo-Gal4 increased Rab11-GFP intensity in FCs. Error bars indicate s.e.m. Scale bar: 5um.

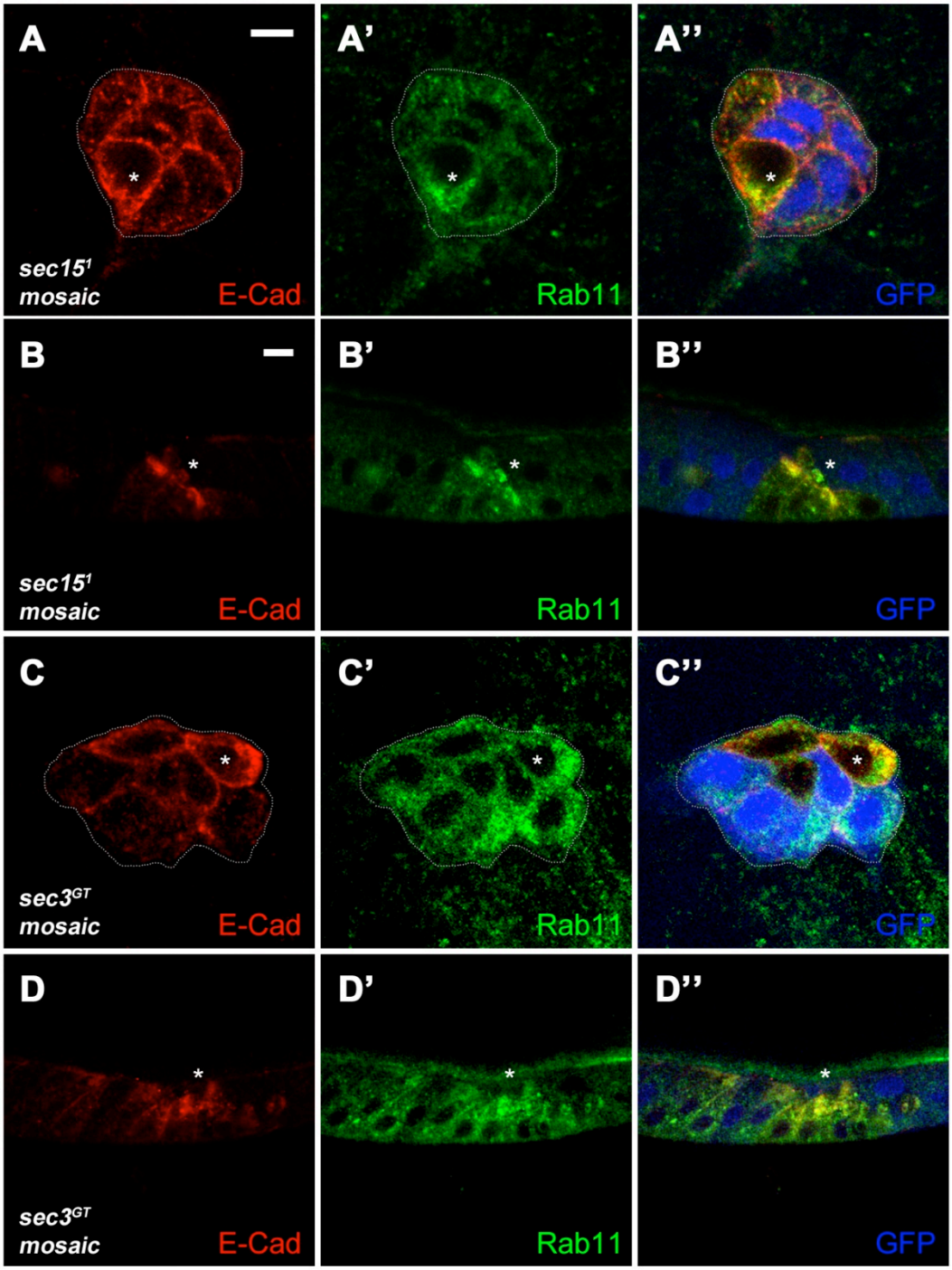

Figure S7. ***sec15*** **mutant cells display similar phenotypes as** ***sec3*** **mutant cells.** (A-B'') E-Cad accumulates in Rab11 marked vesicles in *sec15* [1](Jafar-Nejad et al., 2005) BCs and FCs. (C-D'') E-Cad accumulates in Rab11 marked vesicles in $sec3^{GT}$ BCs and FCs. Mutant cells are marked by * and absence of GFP. Sale bars: 5um.

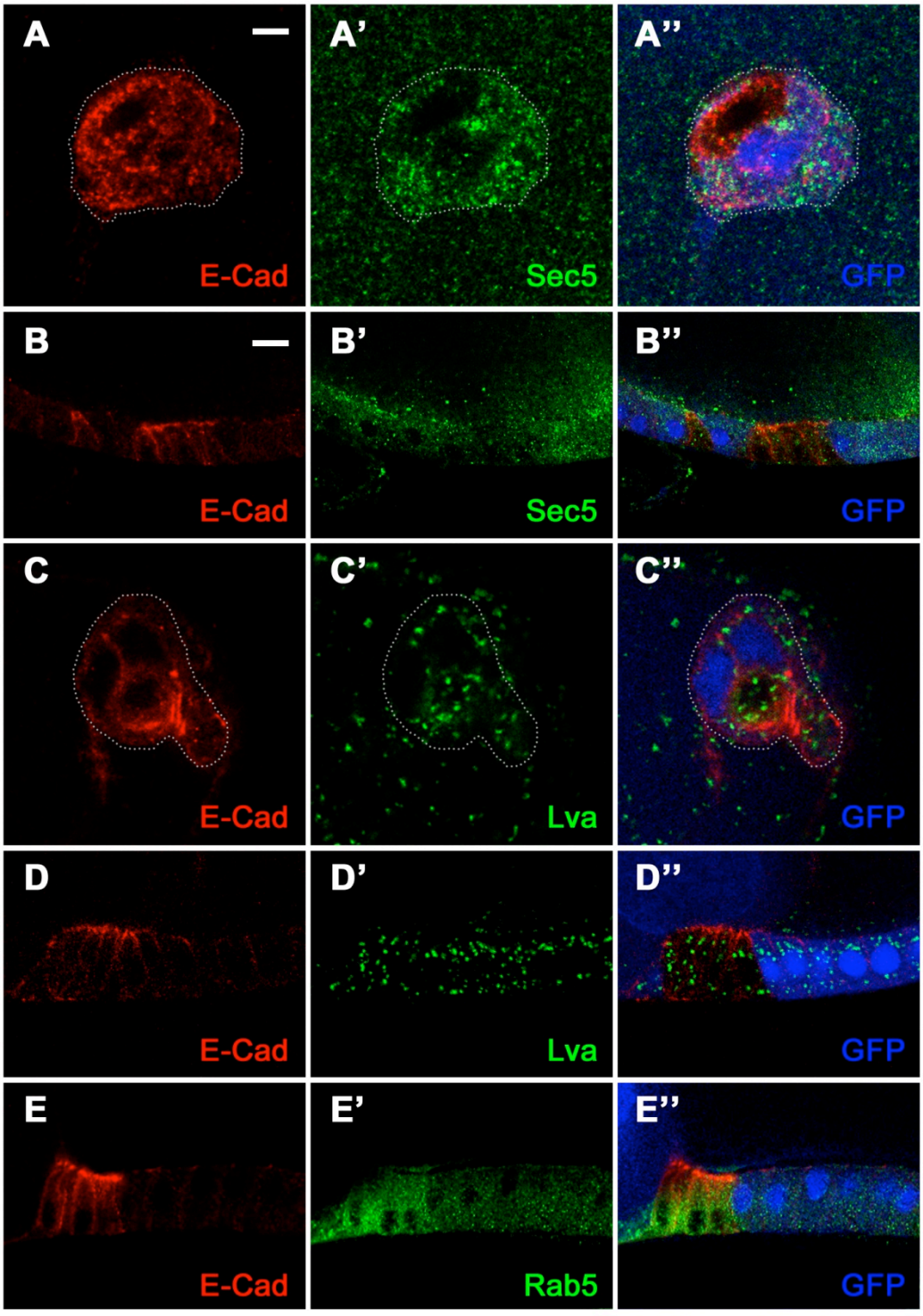

Figure S8. E-cad is not detected in other compartments labeled by Lva and Rab5. (A-B'') *sec3*^{GT} mutant BCs and FCs shows reduced Sec5 signal. (C-D'') *sec3*^{GT} mutant BCs and FCs shows normal distribution of Lva staining, which is and not colocalized with elevated E-Cad staining. (E-E') *sec3*^{GT} mutant FCs shows no siginficant colocalization between Rab5 and E-Cad. The Rab5 signal is elevated in the basal lateral region whereas E-Cad is strongly elevated at the apical cytoplasmic

region. Note that we were unable to obtain good Rab5 stainings in BCs due to antibody penetrability issues. Sale bars: 5um.